Quaternary Science Reviews 249 (2020) 106552

Contents lists available at ScienceDirect

Quaternary Science Reviews

journal homepage: www.elsevier.com/locate/quascirev

# Holocene palaeohydrology of the East Alligator River, for application to mine site rehabilitation, Northern Australia

Mike Saynor [a, *], Robert Wasson [b, d], Wayne Erskine [a, c, 1], Daryl Lam [e]

[a] Environmental Research Institute for the Supervising Scientist, Darwin, Australia
[b] Fenner School of Environment and Society, Australian National University, ACT 0200, Australia
[c] School of Environmental and Life Sciences, University of Newcastle, Ourimbah, NSW 2258, Australia
[d] College of Engineering and Science, James Cook University, Smithfield, Qld, 4878, Australia
[e] Water Technology Pty Ltd, Brisbane, Australia. Level 5, 43 Peel Street, South Brisbane, QLD, 4101, Australia

ARTICLE INFO

*Article history:*
Received 23 April 2020
Received in revised form
5 August 2020
Accepted 17 August 2020
Available online xxx

*Keywords:*
Palaeofloods
Extreme rainfall
Mine site rehabilitation
Mine closure
Northern Australia

ABSTRACT

As a contribution to the estimation of extreme floods and rainfall, palaeofloods in the East Alligator River in tropical Australia were examined to derive estimates of palaeodischarges and their frequency. Nine extreme floods have occurred over 8400 years in a non-stationary series, the youngest five of which are stationary, and the youngest three of which occurred during wet periods produced by variations of the Southern Oscillation Index (SOI) modulated by the Pacific Decadal Oscillation (PDO). The magnitudes of these floods are similar, with one possible exception (in 2007 CE). The extreme floods in the region lie close to, or above, the Australian flood envelope curve showing that floods larger than the expected are possible. Their magnitudes also approximate the Probable Maximum Flood (PMF) but with a much higher frequency than expected. The annual exceedance probability (AEP) of the palaeofloods is 0.3%, which may also be the AEP for the rainfall. These results will be used as input to the design of an artificial landform at the Ranger uranium mine, within the East Alligator catchment, that has to last for 10,000 years. The 2007 CE flood was probably the most extreme flood (and associated rainfall) likely to occur in the vicinity of Ranger under the current climate and will occur in the future along with climate change. Because of the uncertainties associated with projections of future extremes the best design rainfall AEP for the Ranger landform is 0.3%.



## 1. Introduction

The approach adopted here complements existing estimates of extreme rainfall and runoff by investigating palaeoflood deposits to reconstruct palaeodischarge and palaeoprecipitation as input parameters to landform evolution modelling and assessment of the possibility of erosion by flow in Magela Creek of the Ranger uranium mine rehabilitated landform, for which details are provided below. Palaeoflood hydrology is now a well developed field of investigation and is critically important where there are no gauged records or they are too short to reliably capture extremes (Baker, 1987; Benito and O'Connor. 2013; Wilhelm et al., 2018).

While the new data are from the East Alligator River, the results also apply to Magela Creek, a major tributary of the East Alligator (Fig. 1). The rainfall-generating processes are the same in both rivers, largely driven by the position of the monsoon trough (or shear line) in which most tropical lows and cyclones are embedded (Suppiah, 1992; McBride and Keenan, 1982).

Extreme floods have been documented in the Katherine River (Baker and Pickup, 1987; Sandercock and Wyrwoll, 2005; Allen et al., 2020) and in the Koolpin and Jim Jim gorges (Fig. 1), evidenced by sandy slackwater and boulder deposits, producing considerable bedrock scour (Walsh, 1993). Pickup et al., 1987 identified possible slackwater deposits in the East Alligator gorge from aerial photographs and surveys, and a study in a downstream reach of the East Alligator River gorge (referred to hereafter as the 'downstream site') was undertaken by Murray et al. (1992) who described the fluvial sediments as 'slackwater deposits', although they are better described as 'river terrace deposits' (E. Wohl, pers. comm. 2019) derived by floods from upstream. In late February and

* Corresponding author.
*E-mail addresses:* mike.saynor@awe.gov.au, mike.saynor@environment.gov.au (M. Saynor), wasson.robertj@gmail.com (R. Wasson), Daryl.lam@watertech.com.au (D. Lam).
[1] Deceased

https://doi.org/10.1016/j.quascirev.2020.106552
0277-3791/

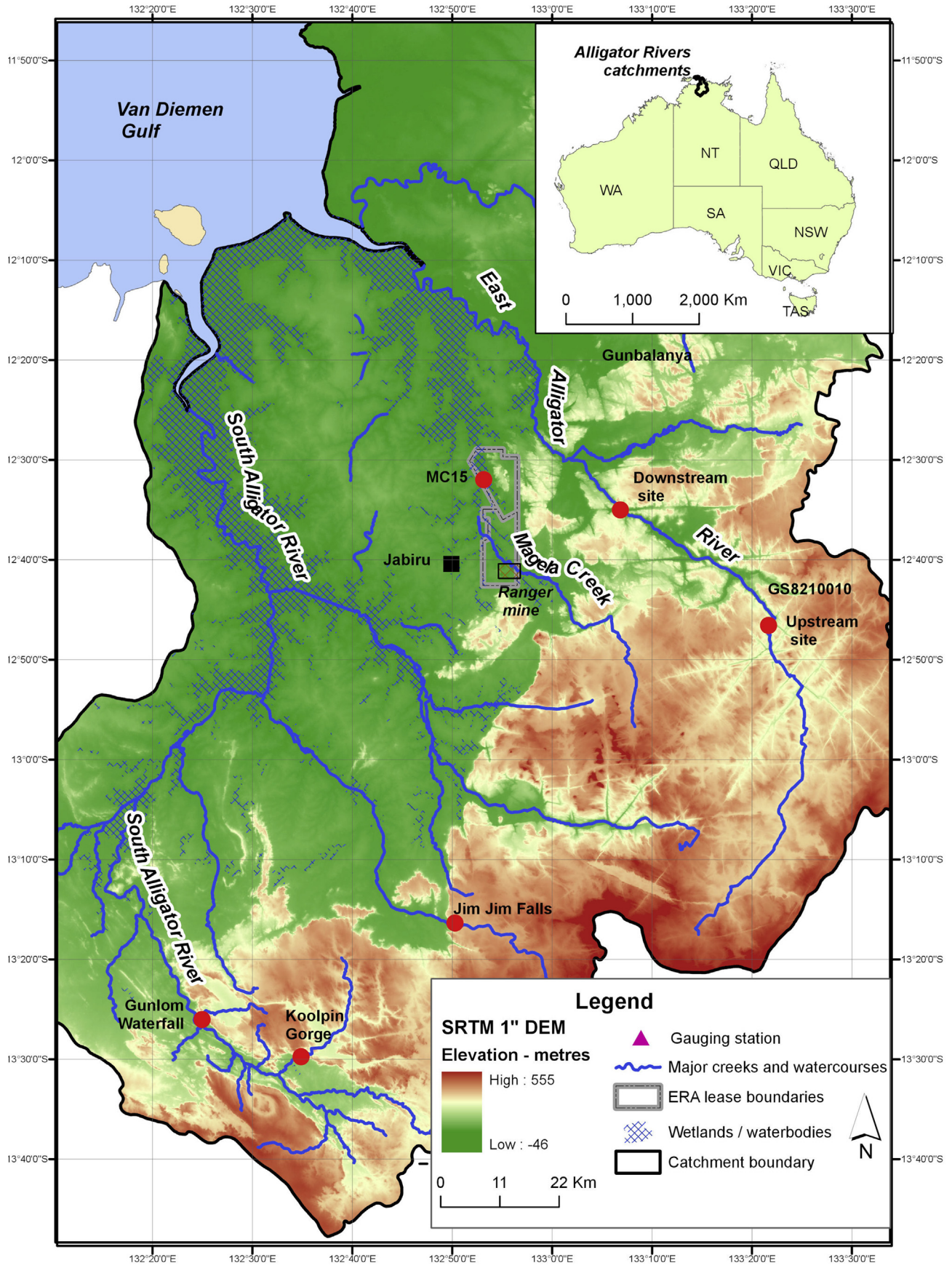


**Fig. 1.** The Alligator Rivers Region showing the East Alligator River catchment, the locations of the upstream and downstream sites, and other locations mentioned in the text.

early March 2007, parts of the East Alligator River catchment (including the Magela Creek sub-catchment) experienced intense rain which resulted in an extreme flood (Erskine et al., 2012; Saynor and Erskine, 2016). For durations greater than 6 h, return periods for rainfall intensities near the Ranger mine exceeded 1:100 years and maximum return periods for 48 and 72 h durations may have exceeded 1:1000 years (Erskine et al., 2012). This flood is hereafter referred to as the 2007 Common Era flood or '2007CE flood'.

Mining has ceased at the Ranger uranium mine (Ranger) in the Northern Territory of Australia (Fig. 1) and the two open cut pits are being backfilled with tailings prior to the construction of a containment landform that will cover the pits and protect the environment downstream, particularly Magela and Gulungul creeks that drain to the World Heritage listed Magela Creek wetlands in Kakadu National Park. In particular, legislated environmental requirements stipulate that the Ranger Project area must be rehabilitated to establish an environment similar to the adjacent areas of Kakadu National Park, such that the rehabilitated area could be incorporated into the Park. One of the main objectives of environmental requirements for the closure of Ranger is that the constructed landform should have "erosion characteristics which, as far as can reasonably be achieved, do not vary significantly from those of comparable landforms in surrounding undisturbed areas" (Australian Government, 1999).

In addition to erosion characteristics, final disposal of tailings must be undertaken on the basis of the best available modelling, in such a way as to ensure that: 'the tailings are physically isolated from the environment for at least 10,000 years' and 'any contaminants arising from the tailings will not result in any detrimental impacts for at least 10,000 years' (Australian Government, 1999).

Modelling of the containment structure to meet these requirements is by means of the landscape evolution models CAESAR-Lisflood and SIBERIA (Coulthard et al., 2000; Hancock et al., 2017), relying on hydro-climatic inputs from short gauged rainfall records, estimates of the probable Maximum Precipitation and Probable Maximum Flood (Bureau of Meteorology, 2011; Water Solutions, 2014), and reconstructions of rainfall and river flow based on a combination of gauged rainfall and flow, and palaeoclimatic reconstructions (Verdon-Kidd et al., 2017). To this can now be added to peak palaeodischarge estimates for most of the Holocene and an estimate of the AEP for the most extreme event in this paper.

## 2. Site description

Despite several low-level surveys by helicopter of the East Alligator River and the adjacent Magela Creek, and noting the evidence of extreme floods in the Koolpin and Jim Jim Gorge gorges (Walsh, 1993) and at the downstream site on the East Alligator River, only one other palaeoflood deposit (hereafter the upstream site; Fig. 1) was identified. The paucity of palaeoflood deposits is possibly because of efficient scouring of flood deposits in the low-sinuosity bedrock gorge (Saynor and Erskine, 2016) where there are few locations for palaeoflood deposits to be preserved.

The catchment area above the GS8210012 gauging station is 2384 $km^2$ (Fig. 1), consisting mostly of the Precambrian Kombolgie Subgroup (specifically the Gumarrirnbang, Marlgowa and McKay Sandstones) which is dominantly a quartz arenite, with some conglomerate and thin siltstone beds and volcanic intervals in the lower part of the Subgroup (Kruse et al., 1994; Polito et al., 2011). These rocks form the western side of the Arnhem Land Plateau, about 200–300 m above sea level, terminating in the Arnhem Land Escarpment that separates the Plateau from the Western Lowlands (CSIRO, 1976). The uppermost member of the Kombolgie Subgroup is the McKay Sandstone which is a quartz-lithic fine-grained sandstone with rip-up mudrock fragments in a silt-size quartzose matrix, and patchy replacement of siliceous cement and mudrock grains by a carbonate mineral (probably dolomite) (T. Munson, pers. comm., 2019). There are also patches of Cretaceous massive and friable sandstone on the Plateau surface (Nott, 1995).

The Plateau rocks are deeply fissured along prominent joints that cause the gorge to have low sinuosity and produce almost straight tributaries. As a result of the quartzose lithology of the Kombolgie Subgroup at the surface of the Plateau, and intense rainfall, the soils according to Aldrick (1976) are very thin to non-existent but with some up to 1.5 m deep in the flattest areas and in depressions. Although there are some areas on the Plateau with sand plains and loamy soils in drainage flats, the catchment of the East Alligator River has none of these and is almost bare of soil. Story (1976) showed that about 45% of the Plateau is bare of vegetation, 39% consists of Sandstone Scrub (heath-like shrubs and spinifex grass), 10% of Sandstone Woodland (scattered eucalypts with members of Sandstone Scrub), and 6% of Tall Open Forest (eucalypts up to 13 m in height).

The mean annual discharge at gauge GS8210010 (Fig. 1) is 1404 Gl (Verdon-Kidd et al., 2017). The study area is in the seasonally wet-dry tropics with a monsoonal climate and distinct wet season from November to March. Mean annual rainfall ranges from 1500mm$yr^{-1}$ at the mouth of the river with values of 1422 mm $yr^{-1}$ at Gunbalanya and 1569 mm $yr^{-1}$ at Jabiru on the Western Lowlands, the two stations closest to both the upstream and downstream sites, and as low as 1000 mm $yr^{-1}$ at the southern end of the catchment (Saynor and Erskine, 2016). Intense rainfall is generated by tropical cyclones and low-pressure systems that emerge from the ocean to the north or from the Gulf of Carpentaria and cross the Plateau. In the 60 years prior to 1975 at least nine cyclones passed over the region, with another eleven passing close enough to produce major rainfall (Hegerl et al., 1982).

The Plateau has been occupied by Indigenous people for at least 48,500 years (David et al., 2019) and perhaps for as long as 65,000 years on the adjacent lowlands (Clarkson et al., 2017) from where foraging on the Plateau may have occurred. Until European arrival less than 200 years ago, land use was dominated by hunting, gathering, and the use of fire to manage resources. There has been little, if any, impact on the Plateau by European uses (Aldrick and Story, 1976; CSIRO, 1976) and the assessment by Larson and Alexandridis (2009) for the entire catchment of 15,875 $km^2$ shows that almost all of it is in a 'natural condition' which is interpreted to mean little impact. It is likely that Indigenous uses had a small effect on vegetation through the use of fire, but little if any impact on soils and runoff as the sandstone is quartz-rich and produces little fine-grain material for soil formation, except for the breakdown of the mudrock fragments and carbonate mentioned above, and therefore the slowing of runoff by water storage. It is reasonable to conclude that the floods in the River have not been affected by land use/land cover change because it is difficult to envisage how any land use could dramatically affect the hydrologic properties of the Plateau given its meagre vegetation and thin to non-existent soils, characteristics that are unlikely to have changed very much over time.

## 3. Methods

### 3.1. Field sampling

The palaeoflood deposits were described in the field from pit faces and auger samples using standard descriptors. These included field texture, the nature of stratigraphic boundaries (almost all were sharp and slightly inclined toward the river, though in augered sections boundaries could only be coarsely described),

types of lamination, compaction, and the presence of charcoal fragments, gravel and bedrock and/or bedrock slabs that may not have been *in situ*. Samples were also taken from one pit for determination of Munsell colours in the laboratory. The charcoal was not subjected to radiocarbon dating because the date for charcoal may have been significantly older than the date of deposition of the sediment that contained the charcoal. This residence time problem can be overcome by dating leaf and/or twig material that is likely to have low residence times (Baker, 1987; Dezileau et al., 2014) but such material was not found in the deposits.

Five pits were excavated, with augering to greater depths in some cases, to document the litho-stratigraphy of the palaeoflood deposits and to sample for Optically Stimulated Luminescence (OSL) dating. All but one of the pits were arrayed either side of a transect across the widest part of the bar (Fig. 2). The highest pit was 1A at about 20 m above the low flow channel and which only reached 1.33 m where bedrock or a large sandstone slab was encountered (Fig. 3). This pit was located about 20 m from the base of the valley wall to avoid sediment introduced from the wall. Pit 1 was about 5 m downslope from Pit 1A and about 0.5 m vertically below Pit 1A, and was limited to a depth of 2.3 m by rock. Pit 3 was about 19 m downslope from 1A, about 18 m above the low flow channel, and reached rock at 2.86 m. Pit 2 was in a shallow runnel, parallel with, and about 14 m above, the river, and by both excavation and augering reached 4.63 m, once again reaching bedrock or a slab of sandstone.

One other pit (Pit 5, Fig. 3) was excavated about 100 m upstream of Pit 1A on the top of the bar and about 1 m vertically below Pit 1, with an excavated depth of 1.15 m and augering to 2.35 m without encountering rock. Samples for OSL were taken from pit faces in light-safe steel tubes, along with additional samples from around each tube for dosimetry. For reasons of timing, the OSL samples were processed in two different laboratories.

### 3.2. Laboratory methods

#### 3.2.1. Dating

For estimating the dates in Pit 1A the following methods were used at the Birbal Sahni Institute for Palaeosciences in Lucknow. Samples were chemically treated with 1 N HCl and 40% $H_2O_2$ to remove carbonates and organic materials respectively. The 90–250 μm grain size fractions from each sample were obtained by dry sieving. Quartz and non-quartz grains were extracted using an isodynamic barrier magnetic separator (LB Frantz Magnetic Separator). Quartz grains were etched using 40% HF and 10% HF respectively for 80 min, followed by HCl treatment (12 N). Grains smaller than 90 μm were discarded by wet sieving. The purity of quartz grains was confirmed from the near background Infra Red Stimulated Luminescence (IRSL) counts from the extracted quartz. Quartz grains (~500 grains) were mounted on stainless steel discs in a monolayer using silicon oil spray. Luminescence measurements were carried out on a Risø TL/OSL Reader TA-20 C/D (Boetter-Jensen et al., 2010) that is equipped with blue (LEDs: 470 ± 30 nm; filtered through GG-420 long-pass filter) and IR (LEDs: 870 ± 40 nm) stimulation sources. IRSL signals were detected by a photomultiplier tube (EMI 9235QA) through the combination of the filters 7.5 mm of Hoya U-340 filter. A calibrated beta source ($^{90}Sr/^{90}Y$) delivering 0.092 Gy $s^{-1}$ was used to irradiate the samples in the reader. The heating rate was 2 °C $s^{-1}$ and the heating was done in an ultrapure nitrogen gas atmosphere. An optimized (using preheat plateau test) value preheat temperature of 200 °C was used. The dose recovery test reproduced a laboratory induced dose of 0.92 Gy within <2%. The concentrations of U, Th and K were measured using an X-ray fluorescence elemental analyzer at the institute of Seismological Research, Gandhinagar, India (Galson et al., 1983). Water content was assumed to be 5 ± 2% for all samples. Dose rates were calculated using a dose rate calculator (DRAC; Durcan et al., 2015). A central age model was used for the oldest date and all other dates were estimated using a minimum age model.


**Fig. 2.** Satellite image from Google Earth™ showing the main features of the upstream slackwater site, the survey line for palaeodischarge calculations, and the locations of the pits in the alluvial deposits. Flow is from left to right.

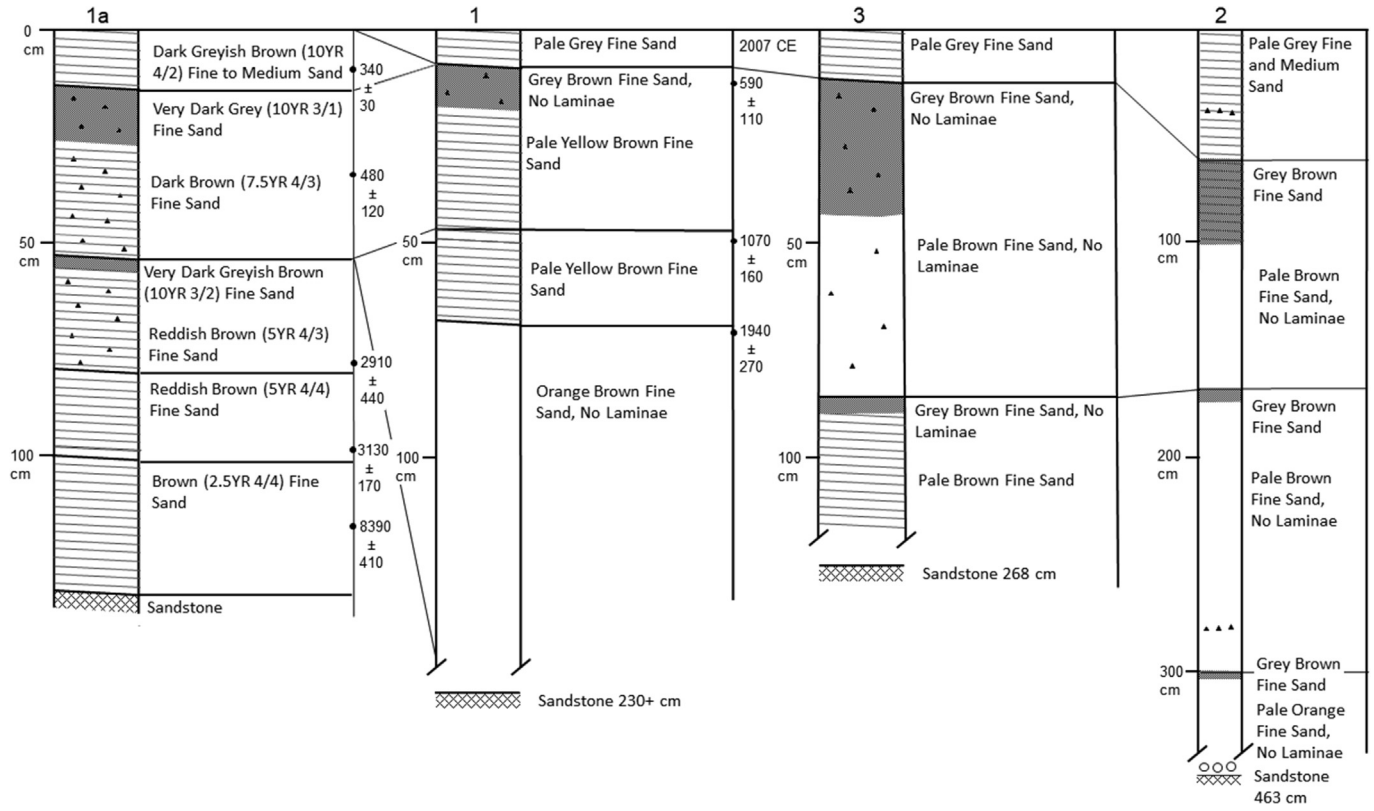


**Fig. 3.** Stratigraphic chart for four of the pits, the locations of which are shown on Fig. 2. Slanting lines are finely laminated sands, the small triangles denote charcoal occurrence, and the circles on top of sandstone in Pit 2 symbolize sub-rounded pebbles.

Analyses of the samples taken from Pit 1 were carried out at the University of Melbourne, using the following method. The samples were processed under subdued red light, with sediment from the light-exposed ends of the tubes discarded. The 180–212 μm quartz fraction was extracted for dating using standard procedures (e.g. Galbraith et al., 1999). Equivalent doses ($D_e$) were calculated using a modified single-aliquot regenerative-dose (SAR) protocol (Murray and Roberts, 1998; Murray and Wintle, 2000; Olley et al., 2004). Approximately 24 small aliquots per sample were preheated at 240 °C for 10s, exposed to infrared (IR) radiation for 50 s at 125 °C to bleach any IR-sensitive signal and optically stimulated for 100 s at 125 °C by blue LEDs attached to an automated Risø TL/OSL-DA-15 apparatus. Ultraviolet luminescence was detected using a photo-multiplier tube with a 7.5 mm U-340 filter. Samples were then given applied doses using a calibrated $^{90}Sr/^{90}Y$ beta-source and re-stimulated to record their regenerative OSL signals. OSL sensitivity changes in the quartz crystals between the natural and regenerative cycles were monitored after each optical stimulation using test doses of 2Gy following a 160 °C cut-heat. Output from the Risø apparatus was analysed using Analyst version 3.21 software (Pirtzel, 2006). OSL data were corrected for any sensitivity changes and dose-response curves constructed using five regenerative dose points. Estimates of equivalent dose were obtained from the intercept of the regenerated dose-response curve with the natural luminescence intensity. Optical ages and their uncertainties were calculated using a minimum age model (Galbraith et al., 1999). K, U and Th concentrations were estimated by instrumental neutron activation analysis (INAA) by Maxxam Analytic and converted to beta dose rates with a beta attenuation factor of 0.88 + 0.03 (Mejdahl, 1979; Adamiec and Aitken, 1998). Gamma dose rates were estimated from radionuclide concentrations measured at Maxxim Analytic, and also using the conversion factors of Adamiec and Aitken (1998) corrected for water content. Internal alpha dose rates were assumed to be 0.03 ± 0.01 Gy $ka^{-1}$ based on previous measurements of quartz from Australia (e.g. Thorne et al., 1999; Bowler et al., 2003). Present-day field moisture contents of the sediments were considered broadly representative of long-term averages and used to correct attenuation of beta and gamma rays by water (Aitken, 1998). Cosmic-ray dose rates were determined from established equations (Prescott and Hutton, 1994).

### 3.2.2. Rainfall estimation

An estimate of the total rainfall for the 2007CE flood was made using radar data from Tindal Airport (about 250 km SSE of the East Alligator River) at 15 locations in the catchment above the gauging station GS8210012, including the upstream slackwater site (Fig. 1). Thiessen polygons were created in a GIS centered on each location and the total rainfall estimated from the sum of catchment polygon areas (2384 $km^2$) was 522 mm for 72 hours. The accuracy of rainfall data declines and is underestimated with distance from the radar station (Chumchean et al., 2004). This effect can be removed by calibration but there are no rainfall stations on the Arnhem Land Plateau that would allow calibration. It is therefore assumed that the rainfall estimate is conservative. River flow data for the 2007CE event were extracted from the Northern Territory Department of Land Resources HRATAB database for gauge GS8210012, for both 72 and 96 h, the latter includes all of the falling limbs of the flood hydrograph.

## 4. The palaeoflood deposits

The upstream deposit is a lateral bar on the right bank of the East Alligator River, in a section of the bedrock gorge that is between 125 and 150 m deep, wider than reaches upstream or

downstream (Fig. 1). There are no other flood deposits in alcoves and on benches on the sandstone cliffs above the lateral bar. Similarly, there are no deposits on the sandstone wall on the other side of the river, but there is a deposit from the latest large flood in 2007 on the footslope on that side of the valley. Given that there are locations on both sides of the valley at levels higher than the lateral bar where flood deposits could have been preserved, and there are none to be found, it seems that the highest deposits in the lateral bar represent the highest flood stages.

The lateral bar at its upstream end begins just downstream from a bedrock ridge that protrudes from the valley wall (Fig. 2). Further downstream the bar widens, as the valley widens, to a maximum width of about 250 m. The bar narrows downstream until it ends about 10 m upstream of bedrock protrusions from both valley walls that constrict low to medium flows with little effect on large flows. The lateral bar in its widest part slopes up from the low flow channel (with local relief of about 1 m) to a height of about 24 m at the base of the cliffs on the valley wall. Thus the bar exists because of a widening of the river, causing a reduction in flow velocity and by the lee effect of the bedrock protuberance at its upstream end. The bar is a type of slackwater deposit where sediment is deposited from suspension, saltation and traction in a channel-margin location where shear stresses are below critical values for transport (Baker, 1987).

The presence of bedrock, or large slabs of sandstone, that have probably not been transported far, at depths of 1–3 m below the surface, suggests that the bar has accumulated on a bedrock footslope and that it is unlikely there are older palaeoflood deposits deeper than those exposed in the pits, with the possible exception of Pit 5. The presence of angular pebble size sandstone clasts at the boundary between the palaeoflood sands and bedrock in Pit 2 (at a depth of 4.55 m) suggests that high shear stresses have occurred across the putative bedrock footslope, producing 'rip-up' clasts.

### 4.1. Litho-chrono-stratigraphy

The OSL dates for the samples from Pits 1 and 1A are provided in Table 1. The stratigraphic units do not display the usual features of flood couplets, namely a sandy base grading upwards to a fine-grained cap (as described and explained by Kale et al., 2010, Wang et al., 2008, and Wasson et al., 2013) but are of approximately uniform texture from top to bottom. Nonetheless, the most plausible explanation of their origin is that they are flood deposits, each produced by a single flood.

There are five flood units in Pit 1A, all of which are compacted and are separated by sharp boundaries slightly inclined towards the river. The youngest unit has fine organic matter dispersed throughout without an identifiable A horizon, but the two units below have rudimentary A horizons shown by organic staining. Most of these and the two oldest units are slightly oxidized as shown by the reddish brown colours, but soil development in these sandy deposits is minimal. All units have millimeter-scale parallel laminations inclined at <5° downstream. Hard charcoal fragments occur in three of the units. The two youngest units date from 1700 to 1500 CE with a break to the next two units that date to about 1000 BCE (Table 1, Fig. 3). The basal unit is much older at about 6400 BCE (Table 1). Angular erosional unconformities were not found in the pit, but the absence of an A horizon in the oldest unit may imply erosion which produced a near-horizontal unconformity. However, the second oldest unit also does not have an A horizon and, given the close correspondence between the age of this unit and the one above, suggests that an erosional unconformity between the two units is unlikely and the absence of an A horizon is not diagnostic of erosion. However, erosion of parts of the sequence cannot be ruled out.

In Pit 1 there are four units, the upper three of which have features like those in Pit 1A except for the youngest unit, which is a loose sand lacking any compaction and minimal organic content. The oldest unit has no laminations, suggesting that it was deposited by rapid deposition from suspension in a flow with a high sediment concentration (Collinson and Thompson, 1989). The topmost unit was deposited by the 2007CE flood as evidenced by its lateral downslope continuity with sand known to have been deposited at that time by comparison of aerial photos and satellite images from 1950CE to 2017CE, and oblique aerial photos taken from a helicopter in June 2006 and May 2007 (Fig. 4). Below this unit is one that correlates both lithologically and chronologically with the second youngest in Pit 1A, but below this unit the dates of about 950 and 80CE, present in Pit 1, are not found in Pit 1A, the most likely cause of which is variations in thickness of the material.

There are only three flood units in Pit 3, the youngest of which is the 2007CE event. Given the complexity of the relationships between Pits 1 and 1A, a correlation between the two older units in Pit 3 and those in Pits 1 and 1A is not attempted. However, it is likely that the two units below the 2007CE unit can be correlated in Pits 3 and 2, but their ages are unknown. Without further OSL dates, for which resources were not available, correlations between the undated and dated pit sequences, apart from the youngest unit formed in 2007CE, would be speculative.

At the top of Pit 5 there is 1.15 m of loose fine to medium sand identical to the units elsewhere attributed to the 2007CE flood. Below this in an auger hole is 0.4 m of grey fine sand, likely to be an A horizon, then 0.55 m of pale brown fine sand overlying a thin layer of grey fine sand that is probably another A horizon, then 0.25 m of pale brown fine sand. There are therefore three flood units at this site, and there may be more below.

## 5. Results and discussion

### 5.1. Flood history

The chronology provided by the OSL dates at the upstream site

**Table 1**
OSL ages from Pit 1 and Pit 1A.

| | ID | De (Gy) | U (ppm) | Th (ppm) | K (%) | Depth (cm) | Age (years BP) | Age (CE/BCE) |
|---|---|---|---|---|---|---|---|---|
| Pit 1 | Nt1-5 | 0.37 ± 0.06 | 0.6 ± 0.1 | 2.2 ± 0.1 | 0.11 ± 0.01 | 15 | 590 ± 110 | 1425 ± 110 CE |
| | Nt5-0 | 0.78 ± 0.09 | 1.2 ± 0.1 | 2.5 ± 0.1 | 0.10 ± 0.01 | 50 | 1070 ± 160 | 950 ± 160 CE |
| | Nt7-5 | 1.38 ± 0.13 | 1.0 ± 0.1 | 2.9 ± 0.2 | 0.12 ± 0.01 | 75 | 1940 ± 270 | 80 ± 270 CE |
| Pit 1A | EALa 1 | 0.22 ± 0.02 | 1.00 ± 0.05 | 1.7 ± 0.1 | 0.07 ± 0.01 | 9 | 340 ± 30 | 1678 ± 30 CE |
| | EALa 2 | 0.36 ± 0.09 | 1.00 ± 0.05 | 3.1 ± 0.2 | 0.14 ± 0.01 | 34 | 480 ± 120 | 1535 ± 120 CE |
| | EALa 3 | 2.36 ± 0.35 | 1.00 ± 0.05 | 4.1 ± 0.2 | 0.17 ± 0.01 | 80 | 2910 ± 350 | 895 ± 350 BCE |
| | EALa 4 | 3.42 ± 0.16 | 1.60 ± 0.08 | 5.1 ± 0.3 | 0.26 ± 0.01 | 97 | 3100 ± 200 | 1120 ± 200 BCE |
| | EALa 5* | 6.69 ± 0.25 | 1.00 ± 0.05 | 4.3 ± 0.2 | 0.22 ± 0.14 | 116 | 8400 ± 400 | 6380 ± 400 BCE |

* Central age model used; all others calculated using a minimum age model.


**Fig. 4.** Oblique aerial photos of the slackwater site reported here taken in June 2006 and May 2007, showing the fresh sand deposited on the right lateral bar sometime between the dates of the photos and that, according to gauged data at GS8210010 (Fig. 1), occurred in March 2007. Flow is from left to right.

shown in Fig. 3 includes a gap between about 895 and 6400 BCE in Pit1A that may be a result of erosional loss of flood deposits by an event or events larger than those that produced the older and younger flood units, or by a highly flashy event that is likely to have been more erosive than a less flashy flood (Reid and Laronne, 1995). Murray et al. (1992) dated fluvial deposits at the downstream site that appear to fill the gap. Therefore, the dates in Fig. 3 and those from Murray et al. (1992) have been combined in Table 2. Most of the chronology presented by Murray et al. (1992) is based on thermoluminescence (TL) dating supplemented by estimates from the excess of $^{226}$Ra over its parent $^{230}$Th, and a few radiocarbon dates. The large uncertainties attached to the TL dates are a result of incomplete bleaching. However, confidence in these ages is provided by the $^{226}$Ra(excess) dates. That said, the relationships between the various dating methods are approximate because of the differences in uncertainties.

The dates in Table 2 are from individual litho-stratigraphic units and their alignment to show likely correlations, between the upstream and downstream sites, is therefore not based solely on dates derived without consideration of stratigraphy. The chronology of the youngest part of the downstream site has not been resolved, and the two TL dates of 790 ± 900 and 690 ± 600 CE appear to be from the same stratigraphic unit (E. Wohl, pers. comm. 2019). The $^{226}$Ra (excess) date of 2400 ± 500 BCE has no TL equivalent and Murray et al. (1992) included it to show order-of-magnitude equivalence with TL dates but it will not be considered further here. In summary, the floods at the upstream site have an approximate equivalent downstream between 950 and 690 CE. The

**Table 2**
TL and $^{226}$Ra(excess) dates (from Murray et al., 1992) and OSL dates from two slackwater sites on the East Alligator River, plus the 2007CE flood at the upstream site.

| Flood Number | OSL dates plus 2007 flood, upstream site | TL dates, downstream site | $^{226}$Ra(excess) dates, downstream site |
|---|---|---|---|
| 1 | 2007 CE | | |
| 2 | 1678 ± 30 CE | | |
| 3 | 1476 ± 80[a] CE | | |
| 4 | 950 ± 160 CE | 790 ± 900[b] CE<br>690 ± 600 CE | 740 ± 200 CE |
| 5 | 80 ± 270 CE | | |
| 6 | 895 ± 440 BCE | | |
| 7 | 1120 ± 170 BCE | | |
| | | | 2400 ± 500 BCE |
| 8 | | 3600 ± 1600 BCE | 3900 ± 600 BCE |
| 9 | 6380 ± 410 BCE | | |

[a] Weighted average of the dates 1535 ± 120 CE and 1425 ± 110 CE in Pits 1 and 1 A respectively.
[b] A radiocarbon date in the same layer has the same age, residence time problems notwithstanding.

upstream floods at about 80CE to 1120 BCE have approximate equivalents downstream, the gap upstream between about 1120 and 6380 BCE is represented downstream by one flood at about 3600 BCE, showing that the upstream gap is of erosional origin. There is no known downstream equivalent of the 6380 BCE flood upstream. In addition, Walsh (1993) reported two radiocarbon dates from charcoal in a sandy slackwater deposit in Koolpin Gorge, which was averaged to a value of 1668 ± 159 CE; about the same age as the second youngest flood at the upstream site and therefore suggesting major flooding in both the East Alligator and South Alligator Rivers at that time. The radiocarbon ages may be older than the deposit because of the residence time effect but this is unlikely, given the small size of the Koolpin Gorge catchment (326 km$^2$).

In combination, the dates from the upstream and downstream sites allow the following conclusions: there have been nine floods large enough to leave a sedimentary record during the past 8400 years (including 2007CE), with an average frequency of 1 in every 930 years. One of these floods, in about 3600 BCE, was either large enough or sufficiently flashy to erode part of the upstream sequence.

A non-parametric runs test was applied to the nine flood ages by transforming their mean ages into yes/no binary data for bins of 100 years, following the method of Wohl et al. (1994). With a $p$ value of 0.4042 it is concluded that the series is non-random, a conclusion also reached by Wohl et al. (1994) for a smaller set of floods from the downstream site. The flood occurrence series is therefore non-stationary.

### 5.2. Palaeofloods and palaeoclimate

If the palaeofloods can be related to specific climatic conditions, particularly large-scale synoptic states such as ENSO (El Niño Southern Oscillation), and the future of these states can be anticipated by climate modeling, then it may be possible to anticipate future floods.

The relationship between floods and past climate states should be based on palaeoclimatic reconstructions either close to the study catchment or applicable to it by means of atmospheric teleconnections. Two reconstructions of high frequency climate changes meet these criteria. The first is a 500-year rainfall reconstruction for Gunbalanya (Fig. 1) (also known as Oenpelli) (Verdon-Kidd and Hancock, 2016) based on a scaling model that matches the variance of the instrumental rainfall record with that of palaeoclimate reconstructions that correlate with the Gunbalanya rainfall record, namely records of the Southern Oscillation Index (SOI), and Nino-3 (see: https://climatedataguide.ucar.edu/climate-data/nino-sst-indices-nino-12-3-34-4-oni-and-tni; accessed 27/6/19), a rainfall index from Great Barrier Reef coral bands, and a 396-year record of rainfall in Southern Jordan (for references to these records see Verdon-Kidd and Hancock, 2016). The reconstructed rainfall was also used in the simple lumped rainfall-runoff model GR1A to reconstruct discharge in the East Alligator River at gauge GS8210010 (Verdon-Kidd et al., 2017).

The most probable ages (i.e. the means) for the three youngest palaeofloods coincide with wet periods in the 500 year rainfall reconstruction, specifically the 2007CE, 1678CE, and the 1476CE floods, although the earliest of these coincides with the beginning of the reconstruction where the full magnitude of the wet period is not known, thereby causing some ambiguity. The uncertainty attached to the OSL estimate of the flood of 1678CE overlaps with the highest reconstructed water year rainfall and runoff, and the above average wet period identified by Verdon-Kidd et al. (2017) from 1650 to 1700CE in the 500-year reconstruction. However, there are wet periods in the 500-year reconstruction for which there are no equivalent palaeofloods, centered at about 1560CE, 1600CE, and 1895CE, possibly because the Gunbalanya rainfall record does not capture all of the spatial variability of rainfall-generating meteorological systems over the East Alligator River catchment. The leading climatic teleconnections that are likely to influence rainfall and so large floods appear to be associated with the Southern Oscillation Index (SOI) modulated by the Pacific Decadal Oscillation (PDO) based on the correlations between these and other palaeoclimatic reconstructions and Gunbalanya rainfall (Table 2 in Verdon-Kidd and Hancock, 2016) and supported by analysis by Wasson and Bayliss (2010).

A second palaeoclimate reconstruction close to the study catchment is in the Magela Swamp in Kakadu National Park, based on the results of Wasson (1992) and Wasson and Bayliss (2010). A 1000-year record of minerogenic and biogenic sedimentation near the upstream end of the Magela Plain was dated by $^{14}$C and $^{226}$Ra(excess), and the minerogenic flux to the Plain was calculated after chemically removing the biogenic component that is clearly autochthonous. The surface of the deposit was bioturbated to a depth equivalent to an average of 40 years of accumulation, and this layer thickness was used for sampling the whole sequence. The minerogenic flux was converted to discharge (in 40-year increments) by assuming that the modern relationship between suspended sediment flux and discharge applies to the whole record. To this has been added the East Alligator flow reconstruction by Verdon-Kidd et al. (2017) with a ten-point moving average (Fig. 5).

Between 1000 and 1120CE the flow was at its highest, then fell to a low at 1400CE. This dry period lasted until 1700CE (1670CE in the higher resolution record of Verdon-Kidd et al., 2017) after which it rose to a higher plateau (but not as high as at the beginning

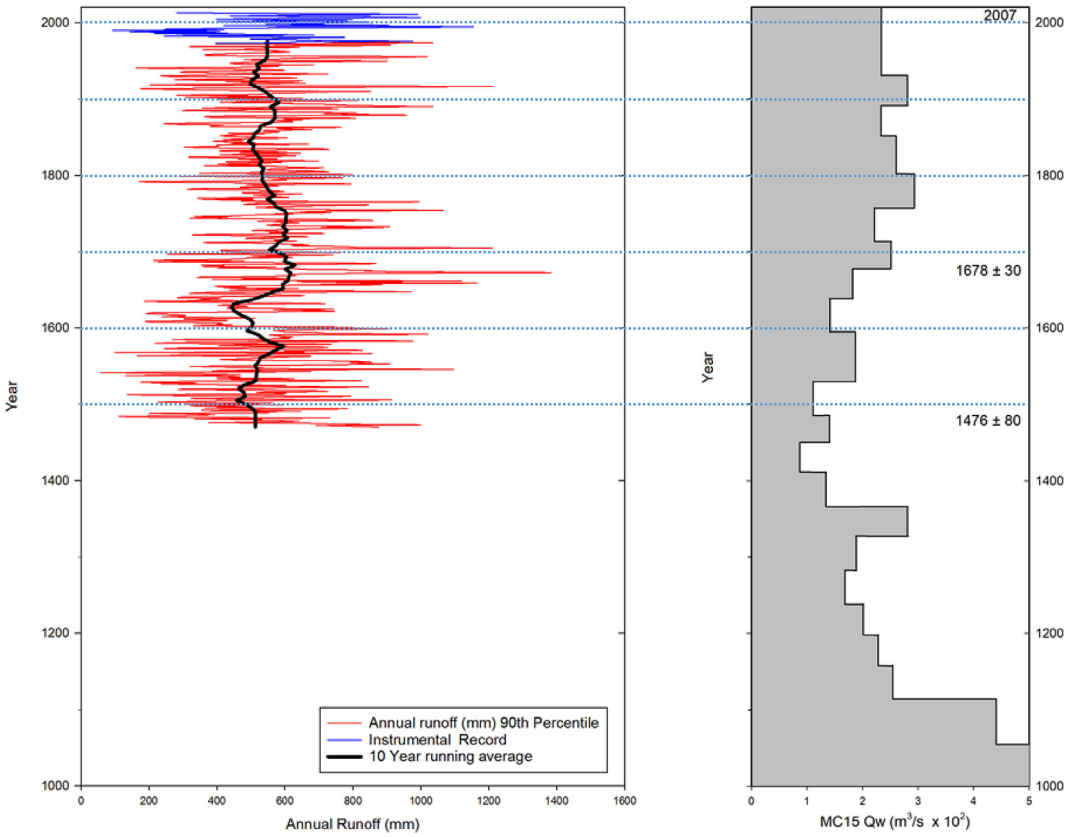


**Fig. 5.** Right panel: Discharge reconstruction at sampling site MC15 on the Magela Plain for the past 1000 years (from Wasson and Bayliss, 2010) with the three youngest of the East Alligator River floods indicated. Left panel: 90th percentile of the water year runoff reconstruction for the East Alligator River with a 10-year moving average (from Verdon-Kidd et al., 2017).

of the record) from about 1760CE (1670CE in the higher resolution record) to the present (Fig. 5). The earliest wet period corresponds to the Medieval Climate Anomaly (MCA), the dry period corresponds to the Little Ice Age (LIA), and the latest period is the Common Warm Period (CWP). The 1477CE flood in the East Alligator River occurred during the LIA and the 1677CE flood occurred at a time of higher average discharge and rainfall. Both of these floods occurred during brief wet periods (Verdon-Kidd et al., 2017), despite their occurrence in broadly different climate states. The 2007CE flood occurred after the Magela record ends but given the results of Verdon-Kidd (2017), it occurred during the latest wet phase that continued after the Magela record ended. Thus, all three floods in the East Alligator River over the past 500 years occurred during wet spells, consistent with the conclusion of Saynor et al. (2012). A longer reconstruction is not available so conclusions can only be reached from the 500-year record.

In relation to low frequency climate changes, the Holocene climate of northern Australia consists of a steady increase of effective precipitation to a maximum between 7000 and 5000 years ago and a sharp decline after 3700 years ago with increased variability after 5000 years ago (Shulmeister, 1999). An annually-resolved record from speleothems in the East Kimberley of Western Australia demonstrates a similar pattern, with an increase in the strength of the Indonesian-Australian Summer Monsoon (IASM) from 9000 to about 4200 years ago, then a sharp decline to a low at 1500 years ago, a peak arid period from 1500 to 1200 years ago, then a rapid increase to 900 years ago that has persisted to the present (Denniston et al., 2013). More relevant to this paper is a detailed record from Girraween Lagoon by Rowe et al. (2019) on the outskirts of Darwin some 200 km west of the East Alligator River which also shows the same pattern. At Gunlom, in the South Alligator River catchment in Kakadu National Park, Nott and Price (1994) documented a doubling of the volume of a plunge pool (Fig. 1) below the Arnhem Land Escarpment between 8000 and 5000 years ago from which they estimated precipitation about twice that of the present day by 5000 years ago. At the exit of Koolpin Gorge, Walsh (1993) used TL to date a floodplain formed by flood flows from the gorge. Most of the deposit was formed at 3500 ± 380 BCE, the weighted average of five overlapping dates coincident with other evidence of a wet period at this time.

The nine palaeofloods in the East Alligator occurred during a period of about 8400 years, during which time effective precipitation had changed, sea level had risen to its Holocene high, and there had been changes in orbital forcing, ENSO variability, the PDO, and teleconnections had strengthened and weakened (McRobbie et al., 2015; Denniston et al., 2013). The palaeofloods did not only occur during low frequency wet periods but also occurred as precipitation increased in the early Holocene, during the Holocene maximum and its subsequent decline, in the driest period, and during the rise of moisture to the present day. The flood series is also non-random, with most floods occurring during the past 3200 years or so, suggesting limited preservation of earlier records, which cannot be discounted given the complexity of the upstream site, or greater flood-generating mechanisms during the period of high climatic variability in the Late Holocene. Another possibility is censoring (Thorndycraft et al., 2005), an unlikely explanation given the small vertical range over which the highest deposits are found.

Whichever explanation holds, the conclusion remains that floods occurred in all states of Holocene climate. In contrast, the coincidence of the three youngest floods with wet spells in the 500

reconstruction of East Alligator River flows shows that high frequency climate variability is more important than low frequency variability. Therefore, it is the state of the SOI (an ENSO indicator) and the PDO that is most important, the basis of the Gunbalanya rainfall and East Alligator flow reconstructions in which the key driver is La Niña (Verdon-Kidd, pers. comm., 2019). When compared with the reconstructed ENSO tendency based on Makassar Straight south-north seawater density (Denniston et al., 2015) the floods at 1678 ± 30CE and 1476 ± 80 CE are at times of high and relatively high La Niña conditions respectively and the flood at 950 ± 160CE occurred when there was a trend to more La Niña conditions. There is no Makassar Straight record of ENSO tendency for the floods in 2007 and 80 ± 270CE, but they occurred when flooding was common in the east Kimberley (Denniston et al., 2015), as did the flood at 950 ± 160CE. The flood at 1476 ± 80CE occurred at the end of a period of high flood frequency in the east Kimberley record, and the flood at 1678 ± 30CE occurred when there is a gap in the Kimberley speleothem record. Based on the results of Verdon-Kidd and Hancock (2016) and Verdon-Kidd et al. (2017) and the comparison with Denniston et al. (2015), it seems that La Niña is the dominant but not exclusive control on extreme floods in the East Alligator catchment.

### 5.3. Estimates of flood discharges

Jarrett and England (2002) provided a summary of the relationships between High Water Marks (HWMs) and the palaeostage indicators (PSIs) for modern floods for rivers with gradients less than 0.002 m $m^{-1}$ and flow depths less than 4.5 m. The average PSI-HWM for 184 observations lies between −0.914 and + 0.457 m, meaning that in some reaches the HWM is lower than the PSI, probably an artefact of data collection. These authors conclude that the top of the PSI is the best estimate of the maximum height of the flood, preferably from sites near the river margin. However, they also suggest that flood height can be estimated by adding to the HWM the average value of PSI-HWM for the particular deposit type. Nevertheless, it is not clear that this procedure can be applied to large flows, as emphasized by the authors. For example, Thorndycraft et al. (2005) show that the HWM was about 1 m higher than the PSI for a flood on the Llobregat River in 2000CE., and Sandercock and Wyrwoll (2005) found evidence of an HWM 3.56 m above the slackwater deposit left by the 1998CE flood in the Katherine Gorge, some 200 km south west of the East Alligator River. These rivers have much greater flow depths than any of those surveyed by Jarrett and England (2002) but generalizing the difference between the PSI and HWM from two sites is not possible, and there does not appear to be any summary of results for rivers as large as the East Alligator. Therefore, the conservative approach of using the top of the PSI as the HWM is adopted, recognizing that there may be a considerable and unquantifiable error attached to this approach.

Because there is only one palaeoflood site, the step-backwater hydraulic modeling method (O'Connor and Webb, 1988), where the gradient of each flood layer is provided by multiple deposits, cannot be used. Therefore, one-dimensional methods have been employed. Two methods have been used to estimate the peak discharges for the palaeofloods. They both rely on measurements of the cross-sectional area and top width of the flow, at the highest palaeoflood stage in Pits 1 and 1 A, and the average gradient of the low flow channel. The first method is based on the modified Chezy equation of Bjerklie et al. (2005):

$$Q = 4.84\, W^{1.1} Y^{1.63} S^{0.33}$$

where Q is discharge, W is top width, Y is mean depth, and S is the channel slope.

From the same authors, the modified Manning equation has been applied:

$$Q = 25.2\, W\, Y^{1.5} S^{0.5}$$

and their regression equation based on discharge measurements in 103 rivers:

$$Q = 4.24\, W^{1.2} Y^{1.63} S^{0.33}$$

The values of Q from the three equations range from 53,918 to 68,158 $m^3\ s^{-1}$ with a rounded mean and standard deviation of 60,600 ± 5800 $m^3\ s^{-1}$. The coefficient of variation of 9.6% for the mean provides some assurance of the accuracy of the estimate even though it is based on a one-dimensional method. Also, while Bjerklie et al. (2005) subjectively excluded from their database rivers with large expansions of flow, which may apply to the study reach of the East Alligator River, the subjectivity does not allow assessment of the importance of this channel form for discharge calculation and therefore has not been taken into account. From this is calculated a mean peak velocity of 9.1 m $s^{-1}$.

The second method to estimate palaeodischarge is based on a berm of sub-rounded boulders of unknown age at the upstream site on the lateral bar about 10 m above the low flow channel. Using Costa's (1983) equation 10, with the mean of the b-axis dimensions of 165 boulders, the minimum velocity required to move them is 3 m $s^{-1}$ which when combined with the cross-sectional area of the valley at that height gives a minimum discharge of 4100 $m^3\ s^{-1}$, assuming that the palaeostage is at the top of the boulders. This is 7% of the peak discharge, calculated above, at the highest palaeostage, showing that the boulders were emplaced at a palaeostage lower than the maximum.

The tops of the palaeoflood deposits in Pit 1A are only 1 m apart vertically, and in Pit 1 only 0.68 m apart. Taking into account the difference in height between Pits 1A and 1 of about 0.50 m, the maximum difference in height of the tops of the deposits is 1.5 m. This is equivalent to an 8% reduction in the cross-sectional area and 11% in the average depth at the upstream site. If it is arbitrarily assumed that there was 1 m of water over the tops of the deposits, this will make a difference to the average bankfull depth of 4% making the total uncertainty about 7% or about 4200 m $s^{-1}$. Adding the uncertainties in the three estimates of the palaeodischarge to these other uncertainties, in quadrature, gives a total uncertainty of 12%. But there are probably other sources of uncertainty, including the errors in topographic survey. Therefore, the most parsimonious conclusion is that the nine palaeofloods of the past 8400 years have been about the same magnitude of 60,600 ± 7300 $m^3\ s^{-1}$ where the uncertainty is probably underestimated, and one flood may have been larger.

### 5.4. Probable Maximum Floods, palaeodischarges and the future

Water Solutions (2014) estimated the Probable Maximum Flood (PMF) for Magela Creek at about 14,400 $m^3\ s^{-1}$ adjacent to the Ranger Mine. Once Pit 3 has been capped the structural integrity of the capping needs to be able to withstand possible scouring, should a PMF occur.

Based on data in Water Solutions (2014) the specific instantaneous peak PMF for Magela Creek is 24.4$m^3 s^{-1} km^2$, and the estimate of mean specific instantaneous peak palaeodischarge for the East Alligator is 25.4 ± 3.0$m^3 s^{-1} km^2$. At Koolpin Gorge the value is 19.9$m^3 s^{-1} km^2$ based on Walsh (1993). While the first two estimates are nearly identical, noting there is no estimate of uncertainty for the PMF for Magela Creek. For Gulungul Creek, which

flows past the western margin of the Ranger mine site, Ramsay (2006) provided data from which a range of specific PMFs has been calculated, from 18.6 to 33.8 $m^3s^{-1}km^2$ for which the Annual Exceedance Probability (AEP) is <1%. This range encompasses those for Koolpin Gorge, Magela Creek and the East Alligator River. The Magela PMF has been calculated from the Probable Maximum Precipitation (PMP) but the average peak flow in the East Alligator takes no account of the PMP, yet they are similar values and fall within the range of the estimates from Gulungul Creek as does that from Koolpin Gorge. No attempt has been made to calculate the PMP for the East Alligator catchment above the upstream site because there are no rainfall gauges on the Plateau.

The differences in the specific PMF estimates for Magela Creek and the Koolpin Gorge may be a result of the use of a rainfall-runoff model for the former and the rational method for the latter to calculate discharges from estimated PMPs, which have been calculated by the same method. The annual exceedance probability (AEP) for the PMF at Koolpin is thought to be more than the 1000-year flood, according to Walsh (1993), and the notional AEP for the Magela PMF is 1-in-$10^6$ years (Water Solutions, 2014). The three catchments are very similar with large areas of bare rock and scant vegetation, in the same climate where intense and prolonged rainfall is generated by tropical lows and cyclones. For example, the 2007CE flood was produced by a slow moving intense low moving to the west within the monsoon trough (http://www.bom.gov.au/watl/about-weather-and-climate/australian-climate-influences.shtml?bookmark=tdexample; accessed 26/05/2019), a common occurrence during the wet season (McBride and Keenan, 1982). The three catchments should behave hydrologically in much the same way, and the identity of the specific Magela PMF and the specific East Alligator flood discharges suggests the same causative mechanism. Nonetheless, why should the mean specific instantaneous peak palaeodischarges in the East Alligator be similar to the PMF in the Magela?

Three explanations are possible. First, the similarity of the specific discharges is a coincidence. Second, the estimates of PMPs from which the PMFs have been calculated are highly inaccurate; Stuart et al. (2016) claim for example that PMPs could have uncertainties of several orders of magnitude (also see Roberts et al., 2016; Wasson, 2016). Third, the PMF is much more frequent than expected according to the notional AEP. It is difficult to assess these options, and certainly there is no known method for testing the accuracy of PMPs and PMFs. If, however, the PMF for the Magela Creek is accepted at face value, the peak flows in the East Alligator Gorge are also accepted, and the three estimates of peak flows are compared with the Australian Envelope Curve (AEC) of Lam et al. (2017), an interesting pattern emerges (Fig. 6). The PMFs for the two smallest catchments lie either on or just above the AEC and the peak floods in the East Alligator are about three times greater than the AEC. Therefore, the AEC does not capture the largest floods and the fact that the East Alligator floods lie above two PMFs in a hydrologically similar region suggests that they are also PMFs.

The AEP for the East Alligator floods cannot be calculated for the entire series because it is non-random. However, the last five floods (since 946CE) are random in time with $p = 0.5$ for a runs test using 50-year bins, and the AEP is 1 in 390 years or 0.3%. The recommended method for converting PMPs into PMFs assumes a probability-neutral transformation from rainfall to runoff, meaning that a rainfall of a given AEP should always result in a flood of the same AEP (Engineers Australia, 2015). According to Roberts et al. (2016), based on guidelines issued by the Queensland Government Flood Commission, for the catchments of Koolpin and the Magela the AEP for the PMP (and therefore the PMF under probability-neutrality) is $10^{-7}$ and about $10^{-6.5}$ respectively, and for the East Alligator about $10^{-5.5}$ (Roberts et al., 2016). The many orders of magnitude difference between these PMP probabilities, the assumed AEP for the Magela PMF of $10^{-6}$ and the AEP for the East Alligator floods could be a consequence of the enormous errors attached to the calculation of PMPs and therefore PMFs. Alternatively, they could be a result of the inadequacies in the calculation of PMPs.

As there is no way of testing PMFs it is assumed that the AEP for the East Alligator floods is correct and all of the others (from Roberts et al., 2016) are under-estimates and, assuming probability neutrality, the AEP for the Magela PMP is also 0.3%. While this conclusion is the best possible at the moment it should be revisited when there is greater clarity about AEP neutrality and the validity of calculations of tropical PMP probabilities (Stuart and Hughes, unpublished; Stuart and Hughes, 2017).

This estimate of the AEP applies to the past, but what is likely to occur in the future when the structural integrity of the artificial landform at Ranger must be maintained? Human-induced climate change is likely to change the frequency of intense La Niñas, the main causal teleconnection for at least the three youngest floods in the East Alligator River. Wang et al. (2017), using a multi-model intercomparison, showed that there is little change of frequency up to a global average temperature increase of 2 °C but that this may double at 4 °C. The timing of such a 4 °C temperature increase is unknown, nor is it clear if this will mean a doubling of extreme floods. While the baseline for future extreme hydroclimatic events has been established in the East Alligator palaeoflood record, which is likely to apply to Magela Creek, there is a very real possibility of a substantial decrease in the return period of 100-year floods (over the next 50–75 years) as climate changes (Hirabayashi et al., 2013). That said, modeling of high, but not necessarily extreme, flows in Kakadu National Park provides ambiguous results; that is, runoff either increased or decreased depending on the selected climate scenario (Léger et al., 2011).

More can be said about the future when sea level change is considered. Bayliss et al. (2018) have modeled sea level change in the Kakadu region to 2100CE where a rise of 1.1 m is estimated. When combined with wet season flooding and a high tide storm surge, these authors show that sea water does not reach the Magela Creek adjacent to the Ranger mine by 2070CE. It is therefore unlikely that there would be any backwater effect of a higher sea level that would increase the stage of fluvial floods near the mine. The longer-term view of Clark et al. (2016) suggests that within the next 3000 years most of the expected global mean sea level increase will have occurred but will not be spatially uniform. According to these authors if the total carbon release is 1280 Pg C, the sea level in the valley of the East Alligator River will be 20–25 m higher than now, impinging on the margins of the artificial landform. If the total carbon release is as high as 5120 Pg C, sea level could rise by 50–55 m which would completely submerge the landform, the top of which is likely to be 44 m above current mean sea level (ERA, 2018). Further modeling to test this possible change of sea level is warranted.

## 6. Conclusions

Nine extreme palaeofloods have been documented in the East Alligator River gorge, occurring over the past 8400 years (including the large flood of 2007CE). Surprisingly, these floods, with one possible exception, are all of about the same magnitude of $60{,}600 \pm 7300$ $m^3 s^{-1}$. The AEP of the youngest (random) part of the flood series is 0.3%. Within this region, where hydrologic behaviour is similar, the specific instantaneous peak discharge of the East Alligator floods and the PMF for Magela Creek are the same, suggesting that all of the East Alligator floods are PMFs, although the

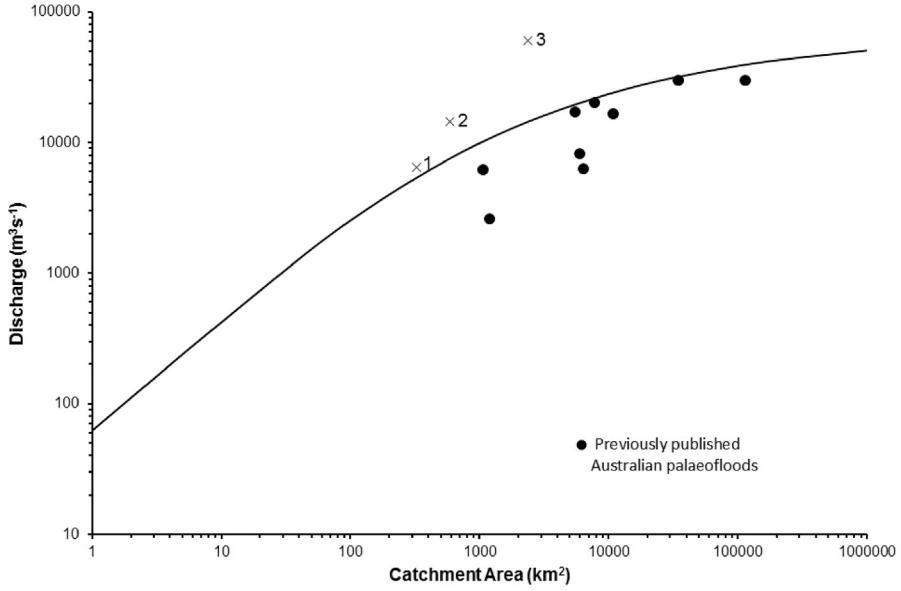


**Fig. 6.** Palaeofloods and PMFs in relation to the Australian Envelope Curve of Lam et al. (2017) from which were also taken the 'Previously Published Australian palaeofloods'. The crosses denote the following sites: 1, Koolpin gorge PMF; 2, Magela Creek PMF; 3, East Alligator gorge palaeofloods.

problems with the calculation of PMFs add uncertainty to this conclusion. The Magela and Koolpin PMFs are close to the Australian Envelope Curve but the peak flows in the East Alligator are about three times larger.

At least the three youngest East Alligator River floods occurred during wet periods produced by variations in the SOI (when the occurrence of La Niña was most important) modulated by the PDO; that is, when the PDO is negative La Niñas are more common. The future of these teleconnections is therefore a key to the future of floods in the region as climate changes. Published climate modeling suggests that a global temperature increase of 4 °C may double the frequency of La Niñas while an increase of 2 °C will have little effect.

The AEP of 0.3% for the East Alligator floods, and also most likely for Magela Creek, and assuming probabilistic neutrality, the best estimate of the PMP at the Ranger site also has an AEP of 0.3%. The rainfall for the 2007CE event, which probably has the same AEP, has already been used in modeling of the artificial landform at Ranger, and further work is likely to take into account the AEP value estimated here (J. Lowry, pers. comm. 2019).

There are many uncertainties attached to these results, including: whether or not all of the East Alligator floods are PMFs and, if they are, why only they are represented in the slackwater deposits; if the AEP of 0.3% is realistic given that it is so much higher than the expected value for PMFs; and if the PMP at Ranger is reliable. The effect of climate change on the putative PMFs has not been assessed, along with the role of a major increase of sea level during the design life of the containment landform at the Ranger mine site. Some of these uncertainties can be reduced by collecting more palaeoflood data, by modeling the runoff system under future climates, and by examining those marine processes that may affect the artificial landform.

## CRediT authorship contribution statement

**Mike Saynor:** Conceptualization, Methodology, Resources, Data curation, Writing - review & editing, Project administration. **Robert Wasson:** Data curation, Formal analysis, Writing - original draft, Writing - review & editing. **Wayne Erskine:** Conceptualization, Methodology. **Daryl Lam:** Validation, Writing - review & editing.

## Declaration of competing interest

The authors declare that they have no known competing financial interests or personal relationships that could have appeared to influence the work reported in this paper.

## Acknowledgements

Three Traditional Owners of the upstream site, Royce Namarnyilk, Greg Lippo and Maath Maralngurru, provided guidance, hard work and good humour and permission to access the sites was given by senior traditional owner Dean Yibarbuk. Mitchel Rudge and Michael Fromholtz of eriss provided field support. John Lowry of eriss provided assistance with Thiessen polygons used for the rainfall estimate for the Plateau for the 2007 flood and also Fig. 1. For various forms of advice, we thank Professor Ellen Wohl of Colorado State University, Dr. Cassandra Rowe of James Cook University, Professor Gerald Nanson of the University of Wollongong, Professor Kurt Lambeck of the Australian National University, Dr. Jamie Stuart of SunWater, and Dr. Danielle Verdon-Kidd of the University of Newcastle who also provided data. Dr Tim Munson, Northern Territory Geological Survey, provided a petrographic description of a specimen from the McKay Sandstone. M. Cupper (Melbourne University) and P. Morthekai (Birbal Sahni Institute for Palaeosciences) are acknowledged for providing OSL dates. Dr Chris Humphrey, Dr Renee Bartolo and Mike Welch of eriss provided helpful comments on a draft of the paper. Ian Fuller and an anonymous reviewer provided useful comments that improved the paper.

## References

Adamiec, G., Aitken, M.J., 1998. Dose-rate conversion factors: update. Ancient TL 16, 37–50.

Aitken, M.J., 1998. An introduction to optical dating: the dating of Quaternary sediments by the use of photon-stimulated luminescence. Oxford University Press, Oxford, p. 267. https://doi.org/10.1017/s0016756899551777.

Aldrick, J.M., 1976. Soils of the Alligator rivers area. In: CSIRO, Lands of the Alligator Rivers Area, Northern Territory. Land Research Series No. 38. Commonwealth Scientific and industrial Research Organization, Australia, pp. 71–88.

Aldrick, J.M., Story, R., 1976. Land use in the Alligator rivers area. In: CSIRO, Lands of

the Alligator Rivers Area, Northern Territory. Land Research Series No. 38. Commonwealth Scientific and industrial Research Organization, Australia, pp. 126–139.
Allen, K.J., Hope, P., Lam, D., Brown, J.R., Wasson, R.J., 2020. Improving Australia's flood record for planning purposes-can we do better? Australas. J. Water Resour. 36–45. https://doi.org/10.1080/13241583.2020.1745735.
Australian Government, 1999. Environmental Requirements of the Commonwealth of Australia for the Operation of Ranger Uranium Mine, pp. 1–11. https://www.environment.gov.au/science/supervising-scientist/publications/environmental-requirements-ranger-uranium-mine.
Baker, V.R., 1987. Paleoflood hydrology and extraordinary flood events. J. Hydrol. 96 (1–4), 79–99. https://doi.org/10.1016/0022-1694(87)90145-4.
Baker, V.R., Pickup, G., 1987. Flood geomorphology of the Katherine Gorge, Northern Territory, Australia. Geol. Soc. Am. Bull. 98 (6), 635–646. https://doi.org/10.1130/0016-7606(1987)98<635:fgotkg>2.0.co;2.
Bayliss, P., Saunders, K., Dutra, L.X.C., Melo, F.C., Hilton, J., Prakash, M., Woolard, F., 2018. Assessing sea level-rise risks to coastal floodplains in the Kakadu Region, northern Australia, using a tidally driven hydrodynamic model. Mar. Freshw. Res. 69, 1064–1078. https://doi.org/10.1071/mf16049.
Benito, G., O'Connor, J.E., 2013. Quantitative paleoflood hydrology. In: Shroder, J., Wohl, E. (Eds.), Treatise on Geomorphology, vol. 9. Academic Press, San Diego, CA, pp. 459–474.
Bjerklie, D.M., Dingman, S.L., Bolster, C.H., 2005. Comparison of constitutive flow resistance equations based on the Manning and Chezy equations applied to natural rivers. Water Resour. Res. 41, W11502. https://doi:1029/2004WR003776.
Boetter-Jensen, L., Thomsen, K.J., Jain, M., 2010. Review of optically stimulated luminescence (OSL) instrumental developments for retrospective dosimetry. Radiat. Meas. 45 (3–6), 253–257. https://doi.org/10.1016/j.radmeas.2009.11.030.
Bowler, J.M., Johnston, H., Olley, J.M., Prescott, J.R., Roberts, R.G., Shawcross, W., Spooner, N.A., 2003. New ages for human occupation and climatic change at Lake Mungo, Australia. Nature 421, 837–840. https://doi.org/10.1038/nature01383.
Bureau of Meteorology, 2011. Generalised probable maximum precipitation estimates for the Ranger tailings dam Hydrometeorological Advisory Service HAS Report No. GTSMR/47, p. 32.
Chumchean, S., Seed, A., Sharma, A., 2004. Application of Scaling in Radar Reflectivity for Correcting Range-Dependant Bias in Climatological Radar Rainfall Estimates. J. Atmos. Ocean. Technol. 21, 1545–1556. https://doi.org/10.1175/1520-0426(2004)021<1545:aosirr>2.0.co;2.
Clark, P.U., Shakun, J.D., Marcott, S.A., Mix, A.C., Eby, M., Kulp, S., Levermann, A., Milne, G.A., Pfister, P.L., Santer, B.D., Schrag, D.P., Solomon, S., Stocker, T.F., Strauss, B.H., Weaver, A.J., Winkelmann, R., Archer, D., Bard, E., Goldner, A., Lambeck, K., Pierrehumbert, R.T., Plattner, G.-K., 2016. Consequences of twenty-first-century policy for multi-millennial climate and sea-level change. Nat. Clim. Change 6, 360–369. https://doi.org/10.1038/nclimate2923.
Clarkson, C., Jacobs, Z., Marwick, B., Fullager, R., 2017. Human occupation of northern Australia by 65,000 years ago. Nature 547, 306–310. https://doi.org/10.1038/nature22968.
Collinson, J.D., Thompson, D.B., 1989. Sedimentary Structures. Unwin Hyman Ltd., London, p. 104. https://doi.org/10.1017/s0016756800006725.
Costa, J.E., 1983. Paleohydraulic reconstructions of flash flood peaks from boulder deposits in the Colorado Front Range. Geol. Soc. Am. Bull. 94, 986–1004. https://doi.org/10.1130/0016-7606(1983)94<986:profpf>2.0.co;2.
Coulthard, T.J., Kirkby, M.J., Macklin, M.G., 2000. Modelling geomorphic response to environmental change in an upland catchment. Hydrol. Process. 14, 2031–2045. https://doi.org/10.1002/1099-1085(20000815/30)14:11/12<2031::aid-hyp53>3.0.co;2-g.
CSIRO, 1976. Lands of the Alligator Rivers Area, Northern Territory. Land Research Series No. 38. Commonwealth Science Industrial Research Organisation, Australia 171.
David, B., Delannoy, J.J., Mialanes, J., Clarkson, C., Petchey, F., Geneste, J.-M., Manne, T., Bird, M.J., Barker, B., Richards, T., Chalmin, E., Castets, G., 2019. 45,610-52,160 years of site and landscape occupation at Nawarla Gabarnmarg, Arnhem Land plateau (northern Australia). Quat. Sci. Rev. 215, 64–85. https://doi.org/10.1016/j.quascirev.2019.04.027.
Denniston, R.F., Wyrwoll, K.-H., Polyak, V.J., Brown, J.R., Asmerson, Y., Wanamaer Jr., A.D., La Pointe, Z., Ellerbroek, R., Barthelmes, M., Cleary, D., Cugley, J., Woods, D., Humphreys, W.F., 2013. A Stalagmite record of Holocene Indonesian-Australian summer monsoon variability from the Australian tropics. Quat. Sci. Rev. 78, 155–168. https://doi.org/10.1016/j.quascirev.2013.08.004.
Denniston, R.F., Villarini, G., Gonzales, A.N., Wyrwoll, K.-H., Polyak, V.J., Ummenhofer, C.C., Lachniet, M.S., Wanamaker, A.D., Humphreys, W.F., Woods, D., Cugley, J., 2015. Extreme rainfall activity in the Australian tropics reflects changes in the El Niño/Southern Oscillation over the last two millennia. Proc. Natl. Acad. Sci. 112 (15), 4576–4581. https://doi.org/10.1073/pnas.1422270112.
Dezileau, L., Terrier, B., Berger, J.F., Blanchemanche, P., Latapie, A., Freydier, R., Bremomd, L., Paquier, A., Lang, A., Delgado, J.L., 2014. A multidating approach applied to historical slackwater flood deposits of the Gardon River, SE France. Geomorphology 214, 56–68. https://doi.org/10.1016/j.geomorph.2014.03.017.
Durcan, J.A., King, G.E., Duller, G.A.T., 2015. DRAC: Dose Rate and Age Calculator for trapped charge dating. Quat. Geochronol. 28, 54–61. https://doi.org/10.1016/j.quageo.2015.03.012.
Engineers Australia, 2015. Australian Rainfall and Runoff. Revision projects. Project 8: use of continuous simulation models for design flood estimation. Project 12: Selection of an Approach 285.
ERA Energy Resources Australia, 2018. Ranger mine closure plan, issued date: may 2018. Revision #: 0.18.0, pp 935.
Erskine, W.D., Saynor, M.J., Jones, D., Tayler, K., Lowry, J.B., 2012. Managing for extremes: potential impacts of large geophysical events on Ranger Uranium Mine, NT. In: Grove, J.R., Rutherfurd, I.D. (Eds.), Managing for Extremes Proceedings of the 6th Australian Stream Management Conference. River Basin Management Society, Canberra, pp. 183–189.
Galbraith, R.F., Roberts, R.G., Laslett, G.M., Yoshida, H., Olley, J.M., 1999. Optical dating of single and multiple grains of quartz from Jinmium rock shelter, northern Australia: Part I, experimental design and statistical models. Archaeometry 41, 339–364. https://doi.org/10.1111/j.1475-4754.1999.tb00987.x.
Galson, D.A., Atkin, B.P., Harvey, P.K., 1983. The determination of low concentrations of U, Th and K by XRF spectrometry. Chem. Geol. 38 (3–4), 225–237. https://doi.org/10.1016/0009-2541(83)90056-6.
Hancock, G.R., Verdon-Kidd, D., Lowry, J.B.C., 2017. Soil erosion predictions from a landscape evolution model - An assessment of a post-mining landform using spatial climate change analogues. Sci. Total Environ. 601-602, 109–121. https://doi.org/10.1016/j.scitotenv.2017.04.038.
Hegerl, et al., Claridge, G.F., Davie, P.J.F., Outridge, P.M., Shanco, P., Stock, E.C., 1982. The Kakadu National Park mangrove forests and tidal marshes: Volume 4, preliminary results of field studies. Australian Littoral Society, Brisbane, p. 32.
Hirabayashi, Y., Mahendran, R., Koirala, S., Konoshima, L., Ymazaki, D., Watanabe, S., Kim, H., Knae, S., 2013. Global food risk under climate change. Nat. Clim. Change 3, 816–821. https://doi.org/10.1038/nclimate1911.
Jarrett, R.D., England Jr., J.F., 2002. Reliability of paleostage indicators for paleoflood studies. In: House, P.K., Webb, R.H., Baker, V.R., Levish, D.R. (Eds.), Ancient floods, Modern Hazards: Principles and Applications of Paleoflood Hydrology, vol. 5. American Geophysical Union, pp. 91–109.
Kale, V.S., Achyuthan, H., Jaiswal, M.K., Sengupta, S., 2010. Palaeoflood records from upper Kaveri river, southern India: evidence for discrete floods during Holocene. Geochronometria 37, 49–55 v10003-010-0026-0">https://doi.org/10.2478/v10003-010-0026-0.
Kruse, P.D., Sweet, L.P., Stuart-Smith, P.G., Wygralak, A.S., Pieters, P.E., Crick, I.H., 1994. 1:250 000 geological map series. Explanatory notes, Katherine SD53-9. Report 1, 69.
Lam, D., Thompson, C., Croke, J., 2017. Improving at-site flood frequency analysis with additional spatial information: a probabilistic regional envelope curve approach. Stoch. Environ. Res. Risk Assess. 31, 2011–2031. https://doi.org/10.1007/s00477-016-1303-x.
Larson, S., Alexandridis, K., 2009. Socio-economic profiling of tropical rivers. Land & Water Australia, Canberra, p. 60.
Léger, L., Ward, M., Andrews, M., Richardson, D., Stewart, J., McKemey, M., Robinson, J., 2011. Kakadu-Vulnerability to climate change impacts. Australian Government, Department of Climate Change and Energy Efficiency 250.
Mejdahl, V., 1979. Thermoluminescence dating: beta-dose attenuation in quartz grains. Archaeometry 21, 61–72. https://doi.org/10.1111/j.1475-4754.1979.tb00241.x.
McBride, J.L., Keenan, T.D., 1982. Climatology of tropical cyclone genesis in the Australian region. J. Climatol. 2, 13–33. https://doi.org/10.1002/joc.3370020103.
McRobbie, F.H., Stemier, T., Wyrwoll, K.-H., 2015. Transient coupling relationships of the Holocene Australian monsoon. Quat. Sci. Rev. 121 https://doi.org/10.1016/j.quascirev.2015.05.011.
Murray, A.S., Roberts, R.G., 1998. Measurement of the equivalent dose in quartz using a regenerative-dose single-aliquot protocol. Radiat. Meas. 29 https://doi.org/10.1016/s1350-4487(98.
Murray, A., Wohl, E., East, J., 1992. Thermoluminescence and excess $^{226}$Ra decay dating of late Quaternary fluvial sands, East Alligator River, Australia. Quat. Res. 37, 29–41. https://doi.org/10.1016/0033-5894(92)90004-3.
Murray, A.S., Wintle, A.G., 2000. Luminescence dating of quartz using an improved single-aliquot regenerative-dose protocol. Radiat. Meas. 32, 57–73. https://doi.org/10.1016/s1350-4487(99)00253-x.
Nott, J., 1995. The antiquity of landscapes on the north Australian craton and the implications for theories of long-term landscape evolution. J. Geol. 103, 19–32. https://doi.org/10.1086/629719.
Nott, J., Price, D., 1994. Plunge pools and paleoprecipitation. Geology 22, 1047–1050. https://doi.org/10.1130/0091-7613(1994)022<1047:ppap>2.3.co;2.
O'Connor, J.E., Webb, R.H., 1988. Hydraulic Modeling for Paleoflood Analysis. In: Baker, V.R., Kochel, R.C., Patton, P.C. (Eds.), Flood Geomorphology. John Wiley and Sons, New York, NY, USA, pp. 393–402.
Olley, J., Pietsch, T., Roberts, R.G., 2004. Optical dating of Holocene sediments from a variety of geomorphic settings using single grains of quartz. Geomorphology 60, 337–358. https://doi.org/10.1016/j.geomorph.2003.09.020.
Pickup, G., Wasson, R., Warner, R., Tongway, D., 1987. A feasibility study of geomorphic research for the long term management of Uranium Mill Tailings. Divisional Report 87/2. CSIRO Division of Water Resources Research, p. 65.
Pirtzel, L., 2006. Analyst Version 3.21. Risø National Laboratory, Roskilde, Denmark.
Polito, P.A., Kyser, T.K., Alexandre, P., Hiatt, E.E., Stanley, C.R., 2011. Advances in understanding the Kombolgie Subgroup and unconformity-related uranium deposits in the Alligator Rivers Uranium Field and how to explore for them using lithogeochemical principles. Aust. J. Earth Sci. 58 (5), 453–474. https://doi.org/10.1080/08120099.2011.561873.
Prescott, J.R., Hutton, J.T., 1994. Cosmic ray contributions to dose rates for

luminescence and ESR dating: large depths and long-term time variations. Radiat. Meas. 23, 497–500. https://doi.org/10.1016/1350-4487(94)90086-8.
Ramsay, R., 2006. Modelling Extreme Floods in the Gulungul Creek Catchment, Northern Territory. BSc Honours Thesis. Charles Darwin University, Darwin.
Reid, I., Laronne, J.B., 1995. Bed load sediment transport in an ephemeral stream and a comparison with seasonal and perennial counterparts. Water Resour. Res. 31 (3), 773–781. https://doi.org/10.1029/94wr02233.
Roberts, M.E., McGuiness, M., Lee, X.J., Whitten, B., 2016. Modelling the probable maximum precipitation for large catchments. Proceedings of the 2015 Mathematics and Statistics in Industry Study Group. https://doi.org/10.21914/anziamj.v57i0.10274.
Rowe, C., Brand, M., Hutley, L.B., Wurster, C., Zwart, C., Levchenko, V., Bird, M., 2019. Holocene savanna dynamics in the seasonal tropics of northern Australia. Rev. Palaeobot. Palynol. https://doi.org/10.1016/j.revpalbo.2019.05.004.
Sandercock, P., Wyrwoll, K.-H., 2005. The historical and palaeoflood record of Katherine river, northern Australia: evaluating the likelihood of extreme discharge events in the context of the 1998 flood. Hydrol. Process. 19 (20), 4107–4120. https://doi.org/10.1002/hyp.5875.
Saynor, M.J., Erskine, W.D., Staben, G., Lowry, J., 2012. A rare occurrence of landslides initiated by an extreme event in March 2007 in the Alligator Rivers Region, Australia. In: erosion and sediment yields in the changing environment. Proceedings of a symposium held at the institute of mountain hazards and environments, CAS-Chengdu, China, 11-15 0ctober 2012. IAHS Publ. 356, 303–310.
Saynor, M.J., Erskine, W.D., 2016. Sand slugs formed by large-scale channel erosion during extreme floods on the East Alligator River, northern Australia. Geografiska Annaler: series A. Phys. Geogr. 98 (2), 169–181. https://doi.org/10.1111/geoa.12131.
Shulmeister, J., 1999. Australasian evidence for mid-Holocene climate change implies precessional control of Walker Circulation in the Pacific. Quaternary International, 57/58, 81-91. https://doi.org/10.1016/s1040-6182(98.
Story, R., 1976. Vegetation of the Alligator rivers area. CSIRO, Lands of the Alligator Rivers Area, Northern Territory. Land Research Series No. 38. Commonwealth Scientific and industrial Research Organization, Australia, pp. 89–111.
Stuart, J., Keogh, R., Hughes, L., 2016. 100 or 10000 year flood, who knows? Implications for dam, floodplain and emergency management. In: Floodplain management association national conference. https://www.floodplainconference.com/papers2016/James%20Stuart%20Full%20paper.pdf.
Stuart, J., Hughes, M., 2017. Atmospheric rivers, cyclones and extreme flood estimation: predicting the location of the next great flood. In: Floodplain Management Association National Conference. http://www.floods.org.au/site/newcastle. (Accessed 30 May 2019).
Stuart, J. and Hughes, M. (unpublished). Variability between Rainfall Runoff Methods and Observed Floods: Implications for Risk, Design, Dam Operation and Communities in Australia. SunWater Ltd., Brisbane.
Suppiah, R., 1992. The Australian summer monsoon: a review. Prog. Phys. Geogr. 16 (3), 283–318. https://doi.org/10.1177/030913339201600302.
Thorne, A., Grün, R., Mortimer, G., Spooner, N.A., Simpson, J.J., McCulloch, M., Taylor, L., Curnoe, D., 1999. Australia's oldest human remains: age of the Lake Mungo skeleton. J. Hum. Evol. 36, 591–612. https://doi.org/10.1006/jhev.1999.0305.
Thorndycraft, V.R., Benito, G., Rico, M., Sopena, A., Sanchez-Moya, Y., Casas, A., 2005. A long-term flood discharge record derived from slackwater flood deposits of the Llobregat River, NE Spain. J. Hydrol. 313, 16–31. https://doi.org/10.1016/j.jhydrol.2005.02.003.
Verdon-Kidd, D., Hancock, G., 2016. Development of synthetic rainfall datasets to enable long-term landform modelling for periods of up to 10 000 years in the Alligator River Region. Unpublished report to the Australian Department of the Environment by the University of Newcastle 33pp.
Verdon-Kidd, D., Hancock, G.R., Lowry, J.B., 2017. A 507-year rainfall and runoff reconstruction for the Monsoonal North West, Australia derived from remote paleoclimate archives. Global Planet. Change 158, 21–35. https://doi.org/10.1016/j.gloplacha.2017.09.003.
Walsh, R.J., 1993. Catastrophic Flood Geomorphology of Two Bedrock Gorges in the Northern Territory, Australia. Unpublished Honours Thesis, Department of Geography. University of Wollongong, p. 82.
Wang, G., Cai, W., Gan, B., Wu, L., Santoso, A., Lin, X., Chen, Z., McPhaden, M.J., 2017. Continued increase of extreme El Nino frequency long after 1.5 °C warming stabilization. Nat. Clim. Change 7, 568–572. https://doi.org/10.1038/nclimate3351.
Wang, Y.-H., Wang, Y.-H., Tang, L.-Q., 2008. On the formation of couplet-style stratifications. Int. J. Sediment Res. 23 (1), 85–91. https://doi.org/10.1016/s1001-6279(08)60008-6.
Wasson, R.J. (Ed.), 1992. Modern Sedimentation and Late Quaternary Evolution of the Magela Creek Plain. Research Report 6, Supervising Scientist for the Alligator Rivers Region. AGPS, Canberra.
Wasson, R.J., 2016. Uncertainty, ambiguity and adaptive flood forecasting. Policy and Society 35, 125–136. https://doi.org/10.1016/j.polsoc.2016.06.002.
Wasson, R.J., Bayliss, P., 2010. River flows and climate in the 'top end' of Australia for the past 1000 years, and the Asian-Australian monsoon. In: Winderlich, S. (Ed.), Kakadu National Park Landscape Symposia Series 2007-2009, vol. 2008, pp. 15–36.
Wasson, R.J., Sundriyal, Y.P., Chaudhary, S., Jaiswal, M., Morthekai, P., Sati, S.P., Juyal, N.A., 2013. 1000-year history of floods in the Upper Ganga catchment, central Himalaya, India. Quat. Sci. Rev. 77, 156–166. https://doi.org/10.1016/j.quascirev.2013.07.022.
Water Solutions, 2014. Report to energy resources of Australia Ltd on ERA Ranger mine pit 3 PMF assessment. In: Document number WS140183, p. 40.
Wilhelm, B., Canovas, J.A.B., Aznar, J.P.C., Kämpf, L., Swierczynski, T., Stoffel, M., Støren, E., Toonen, W., 2018. Recent advances in paleoflood hydrology: from new archives to data comlilation and analysis. Water Security 3, 1–8.
Wohl, E.E., Webb, R.H., Baker, V.R., Pickup, G., 1994. Sedimentary Flood Records in the Bedrock Canyons of Rivers in the Monsoonal Region of Australia. Water Resources Papers, No. 107. Colorado State University, p. 102.